Digital Simulation of Potential Step Experiments Using the Extrapolation Method

ARTICLE *in* ELECTROANALYSIS · DECEMBER 1997

Impact Factor: 2.14 · DOI: 10.1002/elan.1140091806

2 AUTHORS:

Jorg Strutwolf
University of Tuebingen
86 PUBLICATIONS **865** CITATIONS
SEE PROFILE

Wolfgang W Schoeller
Bielefeld University
310 PUBLICATIONS **5,359** CITATIONS
SEE PROFILE

Digital Simulation of Potential Step Experiments Using the Extrapolation Method

*Jörg Strutwolf** + and *Wolfgang W. Schoeller*

Fakultät für Chemie, Universität Bielefeld, D-33501 Bielefeld, Germany
+ Present address: University College, Department of Chemistry, Christopher Ingold Laboratories, 20 Gordon St., London, WC1H 0AJ, UK

Received: June 2, 1997
Final version: September 25, 1997

Abstract
For large values of the model diffusion coefficient the Crank-Nicolson scheme produces poor numerical results, if it is used for the simulation of a potential step experiment. On the other hand the Backward Euler or fully implicit scheme, not suffering from this drawback, is of lower accuracy. We apply the extrapolation method introduced by Morris et al. to the simulation of Cottrellian diffusion and to a simple catalytic mechanism. The extrapolation method, does not show the oscillating behavior of numerical solutions and is of higher accuracy than the fully implicit scheme. Comparison to other implicit difference schemes are presented. The extrapolation schemes show superior results for the diffusional problem and for the short time behavior of the catalytic mechanism.

Keywords: Digital simulation, Potential step experiment, Extrapolation method

1. Introduction

In the mathematical description of a simple potential step experiment a discontinuity between the initial values and the boundary values exists. At time $t \leq 0$ the concentration is homogeneously distributed throughout the region of computation (experimentally throughout the diffusion layer). At $t > 0$ the concentration at the electrode surface is abruptly changed, in case of a potential step to the diffusion limited region, the concentration at the electrode is zero. If finite difference methods are used to solve the diffusion equation, the discontinuity could lead to oscillations of the solution. This was observed in recent publications [1, 2]. The reliable Crank-Nicolson (CN) scheme which is second order accurate in time and the alternating direction implicit (ADI) method show this behavior. In electrochemistry the ADI scheme is applied to calculate the transport to microelectrodes [3–5], i.e., to problems which are two dimensional in space. The ADI scheme is based on splitting of a Crank-Nicolson analogue dicretization formula. To overcome the instability the robust fully implicit (FI) or Backward Euler scheme was used for one dimensional [6] and two dimensional problems [1]. In contrast to the CN algorithm the FI scheme is only first order accurate in time. Richtmyer [7] suggested a three (time) level backward differentiation formula (BDF) to achieve higher accuracy. Three and higher level BDFs were investigated by Feldberg et al. [9, 10] and by Britz [11] with emphasis on electrochemical simulation. One difficulty with BDF modified schemes is the choice of a proper starting protocol. We report the application of an alternative discretization scheme, which is based on the extrapolation of the FI method [12,13]. The extrapolation method does not require starting values and is at least second order accurate in time.

2. Theory

2.1. The Effect of Noncompatible Initial and Boundary Conditions

The physical problem considered is represented by the linear diffusion equation

$$\frac{\partial u(x,t)}{\partial t} = \frac{\partial^2 u(x,t)}{\partial x^2} \tag{1}$$

with boundary and initial conditions

$$t > 0 : u(0,t) = 0, \qquad u(x_{\lim},t) = 1,$$
$$t = 0 : u(x,t) = 1 \quad 0 \leq x \leq x_{\lim}.$$

u, t, x are the variables for concentration, time and space in dimensionless form. The transformation to physical quantities is given in the Appendix (Sec. 6). The maximal value of the space variable taking into account during the computation, $x_{\lim}$, is set to 6 [14]. There is a discontinuity between the boundary condition $u(0,t) = 0$ and the initial value $u(x,0) = 1$ which can be written in vector form $\mathbf{g} = \mathbf{u}(x,0) = (1,1,\ldots,1)^T$.

Using a second order three point finite difference expression to discretize $\partial^2 u/\partial x^2$ produces a system

$$\frac{\mathrm{d}\boldsymbol{v}}{\mathrm{d}t} = \mathbf{A}\boldsymbol{v} + \mathbf{b} \tag{2}$$

where $\boldsymbol{v} = (v_1, v_2, \ldots, v_{N-1})^{\mathrm{T}}$ is the vector of the unknown approximations to $\mathbf{u}$. The $(N-1)$-vector $\mathbf{b}$ contains the boundary conditions, that is the concentrations at $x = 0$ and $x = x_{\lim}$: $\mathbf{b} = \Delta x^{-2}(0,0,\ldots,1)^{\mathrm{T}}$. Δx is the spatial discretization interval and the $(N-1)(N-1)$ matrix is given by

$$\mathbf{A} = \frac{1}{\Delta x^2}\begin{pmatrix} -2 & 1 & & & \\ 1 & -2 & 1 & & \\ & & \ddots & & \\ & & 1 & -2 & 1 \\ & & & 1 & -2 \end{pmatrix} \tag{3}$$

$\mathbf{A}$ is called the diffusion matrix. The theoretical solution of the ordinary differential equation (Eq. 2) for a stepwise evolution in time is [15]

$$\boldsymbol{v}(t + \Delta t) = -\mathbf{A}^{-1}\mathbf{b} + \exp(\Delta t\mathbf{A})(\boldsymbol{v}(t) + \mathbf{A}^{-1}\mathbf{b})$$
$$t = 0, \Delta t, 2\Delta t, \ldots, m\Delta t \tag{4}$$

where $\boldsymbol{v}(0)$ is a vector of initial concentrations. The Padé approximation to the function $\exp(\Delta t\mathbf{A})$ can be used to derive finite difference schemes for the solution of Equation 1 [15–17]. The (1,1)-Padé approximation leads to the familiar CN method

$$\mathbf{c}(t_j + \Delta t) = \frac{\mathbf{I} + \frac{\Delta t}{2}\mathbf{A}}{\mathbf{I} - \frac{\Delta t}{2}\mathbf{A}}\mathbf{c}(t_j) \tag{5}$$

where $t_j = j\Delta t$ ($j = 0, 1, \ldots$). $\mathbf{c}(t_j)$ is a vector approximating $\boldsymbol{v}$ and is

  1040-0397/97/1812-1403 $ 17.50+.50/0

the full numerical approximation to the function u in Equation 1. The constant boundary condition can be incorporated into the rhs vector $\mathbf{c}(t_j)$. $\mathbf{I}$ is the identity matrix. Applying Equation 5 recursively leads to

$$\mathbf{c}(t_j + \Delta t) = \left(\frac{\mathbf{I} + \frac{\Delta t}{2}\mathbf{A}}{\mathbf{I} - \frac{\Delta t}{2}\mathbf{A}}\right)^j \mathbf{g}, \quad j = 1, 2 \ldots, m \tag{6}$$

The (1,0)-Padé approximation results in the FI scheme:

$$\mathbf{c}(t_j + \Delta t) = (\mathbf{I} - \Delta t\mathbf{A})^{-1}\mathbf{c}(t_j), \quad j = 1, 2 \ldots, m \tag{7}$$

The tridiagonal negative definite matrix $\mathbf{A}$ (Eq. 3) has $N-1$ different real and negative eigenvalues λ_i [15]

$$\lambda_i = -\frac{4}{\Delta x^2}\sin^2\frac{i\pi}{2N}, \quad i = 1, 2, \ldots, N-1 \tag{8}$$

The corresponding $N-1$ eigenvectors $\mathbf{w}_i$ are linearly independent and form a basis for the vector of initial values,

$$\mathbf{g} = \sum_{i=1}^{N-1} \alpha_i \mathbf{w}_i \tag{9}$$

α_i are constants. Thus the theoretical solution to Equation 6 for the time $t = t_j$ can be written as

$$\mathbf{c}(t_j) = \sum_{i=1}^{N-1} \alpha_i \left(\frac{1 + \frac{\Delta t}{2}\lambda_i}{1 - \frac{\Delta t}{2}\lambda_i}\right)^j \mathbf{w}_i = \sum_{i=1}^{N-1} \alpha_i R(-\Delta t\lambda_i)^j \mathbf{w}_i,$$

$$j = 1, 2 \ldots \tag{10}$$

At this point we have introduced the amplification factor $R(-\Delta t\lambda_i)$. The amplification factors are determined by the so called stability function $R(z)$ (see [8, 12]) into which one inserts the values

$$z = -\Delta t\lambda_i \tag{11}$$

Note that $z > 0$. In case of the CN method the stability function is given by (see Eq. 10)

$$R(z) = \frac{1 - z/2}{1 + z/2} \tag{12}$$

The stability function describes how each of the $(N-1)$ modes is amplified during one time step.

A similar analysis, starting with the (1,0)-Padé-approximation (Eq. 7) leads to the stability function of the FI scheme

$$R(z) = \frac{1}{1 + z} \tag{13}$$

Lawson and Morris introduced the concept of L_0-stability [12]:

A method is L_0-stable if $\max_{z \geq 0} |R(z)| \leq 1$ and $\lim_{z \to \infty} R(z) = 0$.

A look at the definition of z (Eqs. 11 and 8), and at the stability functions (Eqs. 12 and 13) shows, that the first part of the above definition of stability is fullfiled by the CN and the FI discretization: $|R(z)|$ is always less than one, even for the largest value of z. The value of z is strongly influenced by the model diffusion coefficient $r = \Delta t/\Delta x^2$ (see Eqs. 8 and 11). It follows that the CN and FI schemes are unconditionally stable (for all values of r) or A_0-stable [8, 15]. By the way the stability function for the simple explicit scheme is $R(z) = 1 - z$. This method is not A_0-stable. An inspection of the stability function leads to the stability condition $r \leq 0.5$ for the explicit scheme.

The FI scheme also comply with the second condition of L_0-stability. For growing values of z the function (Eq. 13) approaches zero. However, the stability function for the CN scheme (Eq. 12), shows a different behavior: $\lim_{z \to \infty} R(z) = -1$.

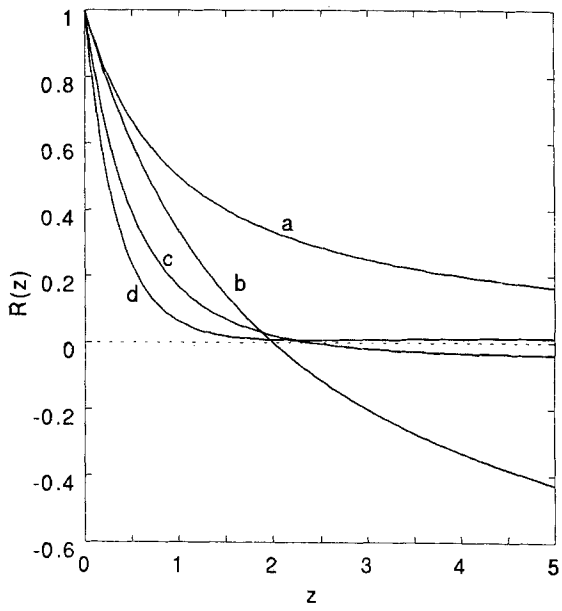

Fig. 1. Stability functions $R(z)$ for the schemes: a) fully implicit (FI), Equation 13; b) Crank-Nicolson (CN), Equation 12; c) second order extrapolation (EXTR-2), Equation 17; d) third order extrapolation (EXTR-3), Equation 22. The variable z is defined by Equation 11.

Though higher accurate in time than FI, the CN scheme is not L_0-stable. The stability function for the FI and CN method are plotted in Figure 1, line a, b, respectively. The lines marked by c and d are stability functions for extrapolation methods which will be treated in the next section. z will be large for the high frequency modes of λ_i $(i = N-1, N-2, \ldots)$ and for large values of the model diffusion coefficient $r = \Delta t/\Delta x^2$. In that case, it is seen from Equations 9 and 10 that components of the initial condition will be preserved at subsequent time steps, but with alternating signs. For smooth initial conditions such an effect may not be noticed, but for noncompatible initial and boundary conditions such discontinuities are preserved and rather distorted than damped out. An illustration

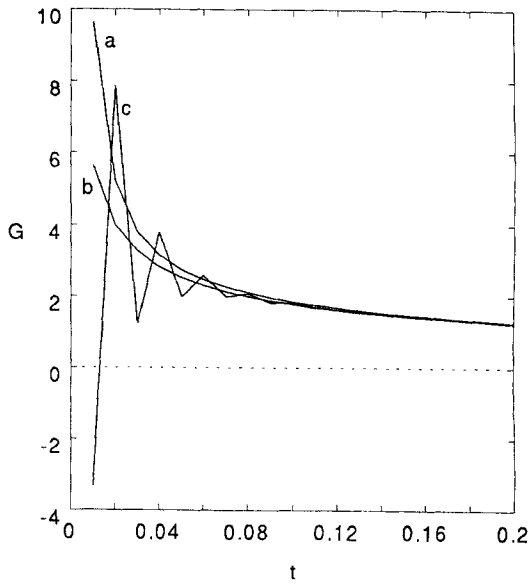

Fig. 2. Dimensionless current–time-plots. a) Cottrell equation in dimensionless form; b) numerical solution using the fully implicit (FI) scheme; c) numerical solution using the Crank-Nicolson (CN) scheme. For the numerical computations the model diffusion coefficient was $r = 2$ and the time step $\Delta t = 0.01$.

of this behavior for the Cottrell problem is given in Figure 2 where dimensionless currents G (cf. Appendix) are plotted against the dimensionless time. Line a is the analytical solution, given by the Cottrell equation in dimensionless form as $G_{ana} = 1/(\pi t)^{1/2}$, line b and c are numerical results using the FI and CN scheme, respectively. The simulation parameters are given in the caption to Figure 2.

To prevent oscillatory solutions one is forced to restrict the value of r by choosing a small time step or a large value of Δx. Lawson and Morris gave an approximate condition for nonoscillating behavior: $\Delta t < 2\Delta x/\pi$ [12]. We found that the second order relation $\Delta t \leq \Delta x^2/2$ [18] is in better agreement with our numerical experiments than the linear relation given by Lawson and Morris.

Results of simulating the Cottrell experiment using the CN scheme are displayed in Figure 3, where the ratio G_{num}/G_{ana} is plotted against the dimensionless time t. $G_{ana} = 1/(\pi t)^{1/2}$ is the dimensionless current, calculated from the Cottrell equation. G_{num} is the numerical result. The simulations in Figure 3 were performed with $\Delta t = 0.001$ and $r = 0.5$, 5, 10 for a, b, c, respectively. From the value of the model diffusion coefficient the spatial step size Δx is forced to be 0.0447, 0.0141 and 0.0100 for a, b and c. For an accurate simulation the relation G_{num}/G_{ana} should almost be one for all values of t. This is seen for simulation a in Figure 3, where the restriction $\Delta t \leq \Delta x^2/2$ is fulfilled ($\Delta x^2/2 = 0.001$). Extensive oscillation is observed for $r = 5$ (b in Fig. 3, $\Delta x^2/2 = 1^{-4}$) and for $r = 10$ (c, $\Delta x^2 = 5^{-5}$). For stiff problems which can arise in electrochemical digital simulations small values of Δx, respectively, large values for r are essential and L_0-stable methods such as the FI scheme are necessary.

In the following section we show the application of the extrapolation method to the numerical solution of the diffusion equation and the extension to a diffusion reaction problem.

2.2. The Extrapolation Method

By combination of the FI scheme applied to different time steps Lawson and Morris [12] obtained a second order accurate in time and L_0-stable algorithm. Consider the following sequence of vectors:

$$\mathbf{c}^{(1)}(t + 2\Delta t) = (\mathbf{I} - 2\Delta t\mathbf{A})^{-1}\mathbf{c}(t) \quad (14)$$

$$\mathbf{c}^{(2)}(t + 2\Delta t) = (\mathbf{I} - \Delta t\mathbf{A})^{-2}\mathbf{c}(t) \quad (15)$$

The binominal expansion of the matrix inverses of Equations 14 and 15 and comparison with the MacLaurin expansion of $\exp(2\Delta t\mathbf{A})$ in Equation 4 shows that neither Equation 14 nor 15 is $O(\Delta t^2)$ accurate. In a linear combination of Equations 14 and 15

$$\mathbf{c}(t + 2\Delta t) = \alpha\mathbf{c}^{(2)} + (1 - \alpha)\mathbf{c}^{(1)} \quad (16)$$

the parameter α can be chosen to achieve second order accuracy. This is the case for $\alpha = 2$ [13]. The stability function for this method is

$$R(z) = \frac{2}{(1+z)^2} - \frac{1}{1+2z} \quad (17)$$

As seen from Figure 1 the scheme is L_0-stable. It is possible to produce higher order L_0-stable methods [13]. For three time steps the following vectors

$$\mathbf{c}^{(1)}(t + 3\Delta t) = (\mathbf{I} - \Delta t\mathbf{A})^{-3}\mathbf{c}(t) \quad (18)$$

$$\mathbf{c}^{(2)}(t + 3\Delta t) = (\mathbf{I} - 2\Delta t\mathbf{A})^{-1}(\mathbf{I} - \Delta t\mathbf{A})^{-1}\mathbf{c}(t) \quad (19)$$

$$\mathbf{c}^{(3)}(t + 3\Delta t) = (\mathbf{I} - 3\Delta t\mathbf{A})^{-1}\mathbf{c}(t) \quad (20)$$

can be combined to

$$\mathbf{c}(t + 3\Delta t) = \alpha\mathbf{c}^{(1)} + \beta\mathbf{c}^{(2)} + (1 - \alpha - \beta)\mathbf{c}^{(3)} \quad (21)$$

Gourlay and Morris have shown, that $\alpha = -\beta = 9/2$ produce a third order accurate scheme whose stability function is

$$R(z) = \frac{9}{2}\left(\frac{1}{1+z}\right)^3 - \frac{9}{2}\left(\frac{1}{1+z(1+2+2z)}\right) + \left(\frac{1}{1+3z}\right) \quad (22)$$

The L_0-stability can be verified from Figure 1. Higher order L_0-stable schemes can be produced [13] but are not treated here.

Besides the simple potential step experiment the first order catalytic mechanism

$$A + e^- \rightleftharpoons B \quad (23)$$

$$B \xrightarrow{k} A \quad (24)$$

was chosen as a test system. The rate constant k has the dimension $1/s$. The system (23) and (24) is expressed by the reaction diffusion equations

$$\frac{\partial u_A(x,t)}{\partial t} = \frac{\partial^2 u_A(x,t)}{\partial x^2} + Ku_B \quad (25)$$

$$\frac{\partial u_B(x,t)}{\partial t} = \frac{\partial^2 u_B(x,t)}{\partial x^2} - Ku_B \quad (26)$$

with initial and boundary conditions

$$t = 0 : u_A(x,t) = 1, \quad 0 \leq x \leq x_{lim},$$
$$u_B(x,t) = 0, \quad 0 \leq x \leq x_{lim}$$
$$t > 0 : u_A(0,t) = 0, \quad u_A(x_{lim},t) = 1,$$
$$\left.\frac{\partial u_A}{\partial x}\right|_{x=0} = -\left.\frac{\partial u_B}{\partial x}\right|_{x=0}, \quad u_B(x_{lim},t) = 0$$

u_A and u_B are normalised concentrations of A and B, respectively. K is the dimensionless rate constant of the homogeneous reaction step (Eq. 24). For the relation between k and K see the Appendix (Eq. 33). The singularities in the boundary and initial conditions should again be noticed. We note that the Reactions 23 and 24 do not lead to a stiff system of partial differential equations. As the scaling time we used the duration τ of the potential step experiment as described

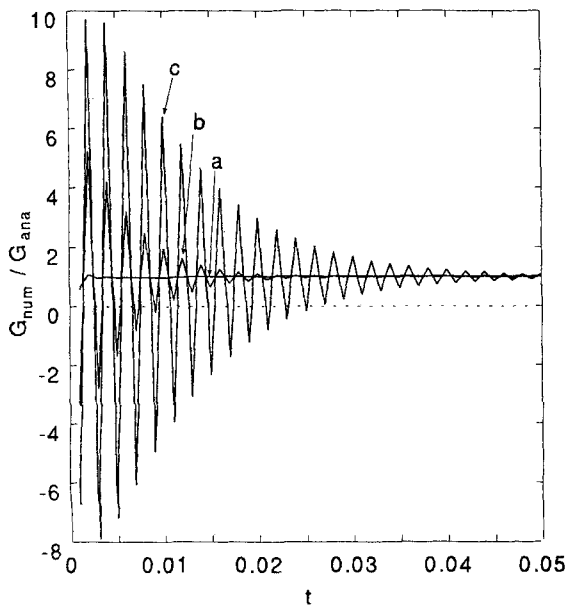

Fig. 3. Oscillating behavior of the numerical solutions of the Cottrell problem due to the L_0-instability of the Crank-Nicolson method. G_{num}/G_{ana} is the ratio of the numerical solution and the dimensionless Cottrell equation. The model parameters for the simulation were $\Delta t = 0.001$ and a) $r = 0.5$ ($\Delta x = 0.0447$); b) $r = 5$ ($\Delta x = 0.0141$); c) $r = 10$ ($\Delta x = 0.0100$).

in the Appendix. For high values of the homogeneous rate constant the system settles down in much shorter time than τ. Because there is no slow decaying species involved, one could use another scaling time, for example the time at which a steady state is reached. However for testing purposes we kept the same scaling time as for the Cottrell problem. This is relevant for reaction schemes where in addition a slow reacting species is present.

The analytical solution of the Equations 25 and 26 is given by [19]

$$G_{ana} = \frac{\exp(-Kt)}{\sqrt{\pi t}} + \sqrt{K}\,\mathrm{erf}(\sqrt{Kt}) \qquad (27)$$

For high values of K a thin reaction layer is formed which thickness is given by $\mu = K^{-1/2}$ [20, 21]. To reduce the required number of concentration points unequal intervals are used. These are generated by application of the transformation function [14, 22]

$$y = \ln(1 + ax) \qquad (28)$$

where a is the expansion factor. This is set to 2 in all simulations. While the intervals in the y-space are equidistant, the transformation (Eq. 28) leads to exponential expanding intervals in x-space.

$$x_i = a^{-1}(\exp(y_i) - 1), \qquad i = 1, \ldots N-1$$

where $x_i = i\Delta x$ and $y_i = i\Delta y$. The smallest x-interval, $x_1 = \Delta x_1$, determines the accuracy of the simulation [14]. The model diffusion coefficient now varies in space and has its critical, i.e., highest value for the first space interval

$$r_1 = \frac{\Delta t}{\Delta x_1^2}$$

Thus in subsequent simulations of the catalytic mechanism r_1 is used as a model parameter.

The coefficient matrix for the catalytic mechanism has a banded structure. To retain the tridiagonal form the system of coupled difference equations is transformed to a block diagonal system which could be solved efficiently [6]. Details of the implementation for the Crank-Nicolson scheme are given by Britz [23]. Modification for the fully implicit and extrapolation method is straightforward.

2.3. Computation

The computations were carried out on a HP 730 workstation, a 32-bit computer, equipped with 86 mb RAM. No bottlenecks such as hard disk access influenced the execution time. The programs were written in Fortran 77 using double precision. They are available upon request from one of the authors (J. S.).

3. Results and Discussion

3.1. Purely Diffusional Problem

We tested the second order extrapolation scheme (EXTR-2), Equations 14–16 and the third order scheme (EXTR-3), Equations 18–21 for different values of the model diffusion coefficient $r = \Delta t/\Delta x^2$. The time step in all calculations was set to 0.001 and an equidistant space grid was used. In Table 1 the error for the current ratio G_{num}/G_{ana} is shown. FIRM-3 is the fully implicit scheme modified with a three-level backward differentiation formula (BDF) as suggested by Richtmyer and Morton [7]. This method was applied recently to electrochemical problems by Mocak and Feldberg [9] and Feldberg and Goldstein [10]. Because of its stability and accuracy FIRM is now the method of choice for simulation of electrochemical systems. For the first iterations the BDFs require concentrations for $t < 0$. We use the starting protocol proposed by Mocak and Feldberg [9], that is setting all starting concentrations equal to their bulk concentrations. Because of the higher accuracy in approximating the derivation with respect to time the FIRM-3 is superior to the FI scheme as can be seen from Table 1. The poorer results for the first time steps for small r are due to inconsistencies of the starting protocol for the BDF. For $r = 5$ the error at $t = 0.006$ (after six time steps) for the CN scheme is due to oscillations which are damped out with progressing time ($t = 0.06$, 60 time steps and $t = 0.6$, 600 time steps). A further increase of r leads to increasing amplitudes of oscillation which are rather amplified than damped out. Finally the initial distortion is continued

Table 1. The error G_{num}/G_{ana} at different times as a function of the model diffusion coefficient r.

	CN	*FI*	*FIRM-3*	*EXTR-2*	*EXTR-3*
r = 0.5					
$t = 0.006$	1.001260	1.091372	1.138333	1.021748	1.014435
$t = 0.060$	1.000506	1.006867	1.004744	1.000848	1.000588
$t = 0.600$	1.000067	1.000693	1.000532	1.000071	1.000068
r = 5					
$t = 0.006$	3.219841	1.069137	0.999193	1.013089	1.010055
$t = 0.060$	1.000047	1.006375	1.004257	1.000365	1.000106
$t = 0.600$	1.000006	1.000632	1.000471	1.000010	1.000006
r = 50					
$t = 0.006$	41.398575	1.068537	1.031894	1.012702	1.008874
$t = 0.060$	23.557140	1.006312	1.004196	1.000304	1.000045
$t = 0.600$	1.000238	1.000626	1.000465	1.000004	1.000001
r = 500					
$t = 0.006$	179.262168	1.068452	1.029875	1.012638	1.008691
$t = 0.060$	405.235530	1.006305	1.004189	1.000298	1.000038
$t = 0.600$	226.604086	1.000625	1.000465	1.000003	1.000000
r = 5000					
$t = 0.006$	616.557766	1.068443	1.029780	1.012432	1.008678
$t = 0.060$	1783.868215	1.006305	1.004189	1.000297	1.000038
$t = 0.600$	4043.376759	1.000625	1.000464	1.000003	1.000000
r = 5 × 10⁴					
$t = 0.006$	1999.502461	1.068442	1.029775	1.012632	1.008677
$t = 0.060$	6156.822067	1.006305	1.004189	1.000297	1.000038
$t = 0.600$	17829.703236	1.000625	1.000464	1.000003	1.000000

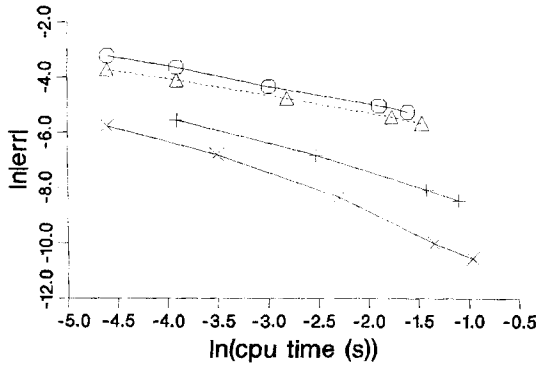

Fig. 4. ln |*err*| in current at time $t = 0.06$ for the simulation of the Cottrellian experiment. $r = 50$, Δt varies from 0.004 to 0.0008. ○: fully implicit scheme (FI); △: fully implicit scheme modified with a three-level backward differentiation formula (FIRM-3); +: second order extrapolation scheme (EXTR-2); ×: third order extrapolation scheme (EXTR-3).

throughout the whole time span. A raise of r from 5 to 5×10^4 leads to a two order decrease of Δx. For problems involving fast homogeneous kinetics one can ensure enough grid points laying inside the reaction layer by choosing an appropriate r. Therefore L_0-stable methods are preferable.

As can be seen from Table 1 EXTR-2 and EXTR-3 are superior to the other methods. A slight drawback is the greater effort of computing time. To progress six time steps the CN, FI and FIRM-3 schemes require six times the solution of the tridiagonal systems (Eqs. 5 and 6), respectively. As can be derived from Equations 14, 15 and 18–20 EXTR-2 requires eight times the solution of a tridiagonal system while EXTR-3 needs ten solutions. This is not too dramatic and is made up by the higher accuracy of the extrapolation schemes, as can be seen from the convergence plots in Figure 4. For decreasing values of Δt, that is increasing number of time steps, the relative error $err = G_{num}/G_{ana} - 1$ for each discretization scheme is calculated and the quantity ln |*err*| is plotted against the logarithm of the cpu-time. For the chosen value of r the CN scheme leads to oscillations and is not represented in Figure 4.

3.2. (Pseudo)first Order Catalytic Mechanism

From the analytical solution (Eq. 27) it follows that a steady state is reached after short time for high values of K or after a longer time for lower values of K. The current is then given by $G_{ana} = \sqrt{K}$. The numerical solution was computed using the CN, FI, FIRM-3 and EXTR-2 schemes.

Table 2 shows the error G_{num}/G_{ana} at different time levels. The dimensionless rate constant and time step chosen was $K = 5$ and $\Delta t = 0.01$. For these parameters 10 concentration sample points falling within the reaction layer allowing an accurate treatment of the homogeneous reaction [14]. For short times the first term of the rhs of Equation 27 dominates and a fast relaxation of the current takes place. For this region the best result is achieved with the EXTR-2 scheme, as can be seen from Table 2 for times $t = 0.04$ and 0.1. Again the poor results of the CN scheme is due to the lack

Table 2. The error G_{num}/G_{ana} for the (pseudo)first order catalytic mechanism at different times. Dimensionless homogeneous rate constant $K = 5$, time step $\Delta t = 0.01$, model diffusion coefficient $r_1 = 5$, expansion factor $a = 2$.

	CN	*FI*	*FIRM-3*	*EXTR-2*
$t = 0.04$	3.715464	1.084591	1.028038	1.025901
$t = 0.10$	1.543407	1.022881	1.009934	1.004410
$t = 0.40$	1.000617	1.001771	1.000844	1.000662
$t = 1.00$	1.000546	1.005764	1.000550	1.000548

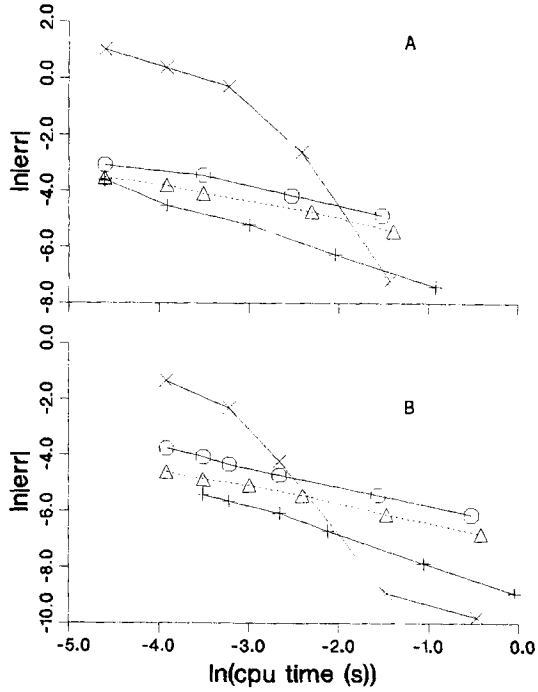

Fig. 5. ln |*err*| in current for the catalytic mechanism. A) at time $t = 0.04$ and B) at $t = 0.1$. Dimensionless homogeneous rate constant $K = 5$, model diffusion coefficient $r_1 = 5$. Δt varies from 0.01 to 0.001. ×: CN, ○: FI, △: FIRM-3, +: EXTR-2.

of L_0-stability. With advancing time the current approaches a steady state and the errors of the CN, FIRM-3 and EXTR-2 methods are getting almost identical. The error for the FI scheme is slightly higher because of the lower accuracy in time. The behavior with respect to the computation time is shown in Figure 5 and 6 where Δt was varied between 0.01 and 0.001. The lines should be compared which each other only within each convergence plot. For short times ($t = 0.04$ and $t = 0.1$, Fig. 5A and 5B, respectively) the EXTR-2 is the most efficient method. For high values of the time step, that is for short cpu times, the CN scheme leads to poor results. For smaller time steps the oscillations are diminished and very accurate results are achieved using the CN scheme. Figure 6A and 6B show the efficiency at $t = 0.4$ and $t = 1$. Here the oscillations due to the L_0-instability of the CN scheme are damped out for all chosen time steps. At $t = 0.1$, Figure 6A, the errors of the EXTR-2, FIRM-3 and CN scheme are similar, but the computation time differs. At $t = 1$ it is clearly seen that the errors of EXTR-2 and FIRM-3 and CN are almost identical, the error of the FI scheme is slightly higher. While the FI, CN and FIRM-3 schemes require the same amount of matrix inversions per time step, the EXTR-2 needs more solutions of the tridiagonal system. The result is a higher effort of computation time as can be seen from Figure 6B.

4. Conclusions

The L_0-stability of a finite difference method is essential for reliable treatment of stiff problems in connection with a discontinuity between initial and boundary values. This situation can occur in simulations of potential step experiments. The very accurate extrapolation method has no restrictions on the time step as a function of the spatial discretization and is well suited to describe short time behavior of potential step experiments. It is preferable to other schemes mentioned here. Furthermore the extrapolation schemes are easy to implement. The emphasis of the present

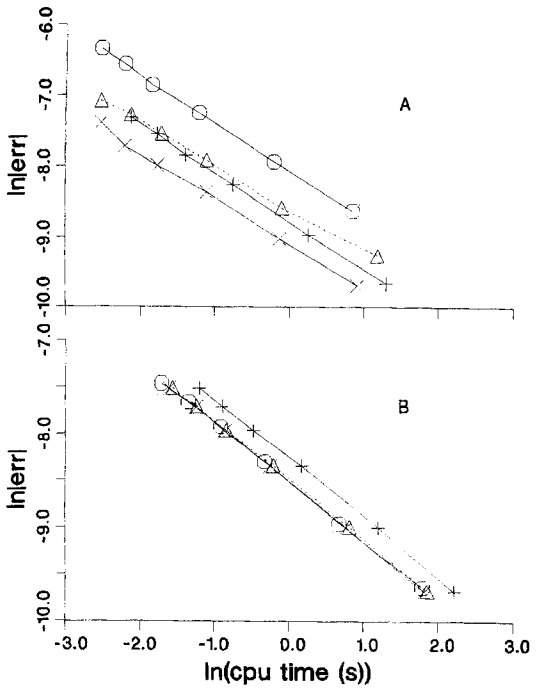

Fig. 6. Same as in Figure 5 but A) at time $t = 0.4$ and B) at $t = 1.0$.

investigation is a comparison with other methods applied to one dimensional diffusion and diffusion reaction problems. An extension to two space variables was done by Lawson and Morris [12]. The application to electrochemical systems involving two dimensional diffusion methods will be the subject of future investigations.

5. Acknowledgement

We thank Prof. W.-J. Beyn, Fakultät für Mathematik, Universität Bielefeld, for valuable discussions.

6. Appendix

6.1. Transformation to Dimensioned Variables

All computations were done with dimensionless variables c, t, x, G, K. The transformations to physical variables (in the following marked with an overbar) are

Concentration

$$\bar{c}_x = \frac{c_x}{\bar{c}_A^{\,b}}, \qquad x = A, B \tag{29}$$

$\bar{c}_x$ concentration of species x [mol/cm^3], $\bar{c}_A^{\,b}$ bulk concentration of A.

Time

$$\bar{t} = t\tau \tag{30}$$

$\bar{t}$ time [s], τ duration of the experiment [s].

Space

$$\bar{x} = x\sqrt{D\tau} \tag{31}$$

$\bar{x}$ space [cm], D diffusion coefficient [cm^2/s] ($D_A = D_B$ is assumed).

Current

$$\bar{i} = nFA\bar{c}_A^{\,b}\sqrt{D/\tau}G \tag{32}$$

$\bar{i}$ current [A], A the area of the electrode [cm^2]. F and n have their usual meaning.

Homogeneous rate constant

$$k = K/\tau \tag{33}$$

k first order rate constant [1/s].

7. References

[1] J.A. Alden, R.G. Compton, *J. Electroanal. Chem.* **1996**, *402*, 1.
[2] D. Britz, *J. Electroanal. Chem.* **1996**, *406*, 15.
[3] J. Heinze, *J. Electroanal. Chem.* **1981**, *124*, 73.
[4] J. Heinze, M. Störzbach, *Ber. Bunsenges. Phys. Chem.* **1986**, *90*, 1043.
[5] G. Taylor, H.H. Girault, J. McAleer, *J. Electroanal. Chem.* **1990**, *293*, 19.
[6] M. Rudolph, *J. Electroanal. Chem.* **1991**, *314*, 13.
[7] R.D. Richtmyer, K.W. Morton, *Difference Methods for Initial Value Problems*, 2nd ed., Interscience, New York **1967**.
[8] E. Hairer, G. Wanner, *Solving Ordinary Differential Equations II. Stiff and Differential-Algebraic Problems*, Springer-Verlag, Berlin **1991**.
[9] J. Mocak, S.W. Feldberg, *J. Electroanal. Chem.* **1994**, *378*, 31.
[10] S.W. Feldberg, C.I. Goldstein, *J. Electroanal. Chem.* **1995**, *397*, 1.
[11] D. Britz, *Comput. Chem.* **1997**, *21*, 97.
[12] J.D. Lawson, J. Ll. Morris, *SIAM J. Num. Anal.* **1978**, *15*, 1212.
[13] A.R. Gourlay, J. Ll. Morris, *SIAM J. Num. Anal.* **1980**, *17*, 641.
[14] D. Britz, *Digital Simulation in Electrochemistry*, 2nd ed., Springer-Verlag, Berlin **1988**.
[15] G.D. Smith, *Numerical Solution of Partial Differential Equations: Finite Difference Methods*, 3rd edn., Oxford University Press, Oxford **1985**.
[16] R.S. Varga, *Matrix Iterative Analysis*, Prentice-Hall, Englewood Cliffs, New Jersey **1962**.
[17] M.K. Jain, *Numerical Solution of Differential Equations*, Wiley Eastern Limited, New Delhi **1979**.
[18] W.L. Wood, R.W. Lewis, *Int. J. Num. Meth. Engng* **1975**, *9*, 679.
[19] P. Delahay, G.L. Stiehl, *J. Am. Chem. Soc.* **1952**, *74*, 3500.
[20] K.J. Vetter, *Elektrochemische Kinetik*, Springer-Verlag, Berlin **1961**.
[21] D. Britz, *J. Electroanal. Chem.* **1988**, *240*, 17.
[22] S.W. Feldberg, *J. Electroanal. Chem.* **1981**, *127*, 1.
[23] D. Britz, *J. Electroanal. Chem.* **1993**, *352*, 17.